CME LIVE OPEN ACCESS

Journal of
Theoretical Physics & Mathematics Research

Review Article

Interpretation of Self-Potential Anomaly Due to a New Model Using Complex Gradient.

Aram Moradi*

Department of Physics, University of Alberta Edmonton, Canada

***Corresponding Author:** Aram Moradi, Department of Physics, University of Alberta Edmonton, Canada

Received: 2023 Dec 04 **Accepted:** 2023 Dec 25 **Published:** 2024 Jan 15

Abstract

Complex Gradient Method is a fast and straight-forward method of estimating origin parameters of self-potential anomaly using SP data horizontal and vertical derivatives simultaneously. Here, it is assumed that SP anomaly mass is a two-dimensional inclined sheet whose parameters are depth to upper edge, depth to bottom edge, dip angle and electrical dipole moment. The complex gradient method validity is proven by applying it to synthetic data, with and without adding noise, for cases in which some parameters are constant while others are variable. The method is also applied to estimate model parameters for field data in three zones of a copper mine in the Surda region of India, a copper sulfide mine in Suleymankoy, Turkey, and a graphite mine in Southern Bavarian in Germany. Comparing the results of the latter case with those of other methods indicate that the complex gradient method well identifies the parameters of self-potential source and mistakes were corrected in the same article.

Keywords: Sp, Two-Dimensional Inclined Sheet, Complex Gradient, Depth, Electric Dipole Moment, Dip Angle.

1. Introduction

In some parts of the ground, when two electrodes are at certain distances from each other, there is naturally a measurable potential difference between them called the spontaneous potential which results from electrochemical reactions between minerals and solutions in contact with them. Self-potential or Sp method is one of the oldest electrical methods. In this method, electrical current does not enter the ground from outside, but it is the ground natural current that is used. Among self-potential method applications are the exploration of metal sulfides, oil fields, water exploration, mining exploration, geothermal, archaeological, sea floor mineral, and deposit assessment to investigate earthquakes and volcanic eruptions [1-8]. A good way to interpret SP anomalies is to use simple shapes such as inclined sheets. Among the models used so far to interpret SP anomaly reason include spherical and vertical cylinders, horizontal cylinders, inclined plate, inclined sheets, and inclined sheet here [9-12]. The two-dimensional inclined sheet is considered as the SP anomaly reason and the main purpose is to determine the parameters of depth to upper edge, depth to bottom edge, electric dipole moment and angle of dip related to inclined sheet. In complex gradient method, horizontal gradient is calculated by numerical derivative method. Then, vertical gradient is calculated by analytical signal and Hilbert transform of horizontal gradient. By multiplying the vertical gradient by i and its sum by the horizontal gradient, the complex gradient is calculated.

1.1. The Concept of Self-Potential

Figure 1 shows a two-dimensional inclined sheet model in which h represents the depth to upper edge, H the depth to bottom edge, L the length of sheet, r_1 and r_2 the upper edge distance and bottom edge from the measuring point P along x-axis, b the length of horizontal projection of inclined sheet on the ground surface, K the electric dipole moment and θ the dip angle of the sheet. Horizontal extension of this inclined sheet (outwards or inwards) is infinite. That is why it is considered as two-dimensional. In the article entitled "A New Approach to Interpret Self-Potential Anomaly Aver a Two-Dimensional Inclined Sheet Using Complex Gradient Analysis", the authors did the same thing, but the formulas for model parameters were set incorrectly and did not match the results; consequently, the resulting horizontal gradient diagram was incorrectly plotted due to incorrect mathematical formulas. In this paper, the formulas are modified and correct diagrams have been plotted [12].

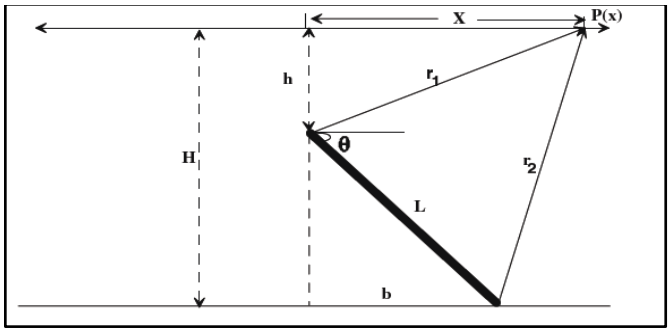

Figure 1: Cross Section of an Inclined Sheet of Finite Depth Extent.

For potential anywhere, we have x_i [13]:

$$V(x_i) = Kln\left(\frac{r_1^2}{r_2^2}\right), \text{ i=1,2, 3..., N (1)}$$

Now according to Figure (1):

$$r_1 = \sqrt{x_i^2 + h^2} \quad , \; r_2 = \sqrt{(x_i - b)^2 + H^2} \quad , \qquad b = \frac{H-h}{\tan\theta}$$

Where at x_i=0 the potential is:

$$V(0) = Kln\left(\frac{h^2}{b^2+H^2}\right) \quad (2)$$

The complex gradient $V_c(x)$ which is equal to the sum of horizontal gradient and vertical gradient, is calculated as follows:

$$V_c(x) = \frac{\partial V(x)}{\partial x} + i\frac{\partial V(x)}{\partial z} \quad (3)$$

Derived from (1) to x and z we have:

$$V_x(x) = \frac{\partial V(x)}{\partial x} = 2K\left[\frac{x}{x^2+h^2} - \frac{(x-b)}{(x-b)^2+n^2h^2}\right] \quad (4)$$

$$V_z(x) = \frac{\partial V(x)}{\partial z} = 2K\left[\frac{h}{x^2+h^2} - \frac{n^2h}{(x-b)^2+n^2h^2}\right] \quad (5)$$

Here, z is the same as h and we consider H=nh, but in the article had yield [12]:

$$V_z(x) = \frac{\partial V(x)}{\partial z} = 2K\left[\frac{h}{x^2+h^2} - \frac{nh}{(x-b)^2+n^2h^2}\right].$$

Also in self-potential anomaly, the relationship between horizontal and vertical gradients is given as follows:

$$V_x(x) \overset{HT}{\leftrightarrow} -V_z(x) \quad (6)$$

HT means Hilbert transformation. The unknown parameters in Equation (1) which include *K, H, h, θ, b* are obtained by applying the following conditions:

1) The distance of the zero anomaly (x_0) is the distance from origin to the point where V(x)0. After equation (1), x_0 is calculated as follows:

$$x_0 = \frac{b^2+h^2(n^2-1)}{2b} \quad (7)$$

2) The points of the horizontal gradient are the points where V_x (x)=0. Thus, by setting Equation (4) equal to zero, the following equation can be obtained:

$$x^2 - \frac{x[b^2+h^2(n^2-1)]}{b} - h^2 = 0 \quad (8)$$

In the mentioned article, formula (8) is obtained as

$$x - \frac{x[b^2+h^2(n^2-1)]}{b} - h^2 = 0.$$

Using equation (7) in equation (8), the following equation is obtained

$$x^2 - 2x_0x - h^2 = 0 \quad (9)$$

By solving the above equation, its two roots are obtained as follows:

$$x(max) = x_0 + \sqrt{x_0^2 + h^2} \quad (10)$$

$$x(min) = x_0 - \sqrt{x_0^2 + h^2} \quad (11)$$

Therefore, x(max), x(min) are the points where horizontal gradient is zero V_x (x)=0 and after combining the two roots, the depth to the upper edge parameter of the sheet can be obtained:

$$h = |\, x(max).x(min)|^{\frac{1}{2}} \quad (12)$$

3) Zero vertical gradient points where V_z (x)=0. So, by V_z (x)=0 the following equation is obtained:

$$(1-n^2)x^2 - 2bx + b^2 = 0 \quad (13)$$

In the mentioned article, Formula (13) is obtained as:

$$(1-n)x^2 - 2bx + b^2 + h^2(n^2-n) = 0$$

By solving Equation (13), its roots are obtained. Then, by combining these two roots, Equation (14) will be obtained:

$$x_1 = \frac{b+bn}{(1-n^2)}, \quad x_2 = \frac{b-bn}{(1-n^2)} \quad (14)$$

$$x_1 + x_2 = \frac{2b}{1-n^2}$$

Therefore, x_1, x_2 are the points where vertical gradient is zero. Now using (7) and (14), n will also be obtained:

$$n = \sqrt{\frac{(x_1+x_2)^2 - 4x_0(x_1+x_2) - 4|\, x(max).x(min)|}{(x_1+x_2)^2}} \quad (15)$$

In the Article (Hafez and Abbas, 2009) is

$$n = \left|\frac{(x_1+x_2)^2 - 4x_0(x_1+x_2) - 4|\, x(max).x(min)|}{(x_1+x_2)^2 + 4[x(max).x(min)]}\right|$$

By determining n, the depth to bottom edge parameter is obtained [12]:

H=nh (16)

Sing the following Equation (16) from Equation (7), parameter b is:

$$b = x_0 + \sqrt{x_0^2 - h^2(n^2-1)} \quad (17)$$

In the article, this parameter is

$$b = x_0 - \sqrt{x_0^2 - h^2(n^2 - 1)}\,.$$

Now according to Figure (1), the dip angle is obtained from the following equation:

$$\theta = \tan^{-1}\frac{H-h}{b} \qquad (18)$$

The electric dipole moment is also calculated by solving Equation (4) at the origin, x=0

$$K = \frac{(b^2+H^2)V_x(0)}{2b} \qquad (19)$$

By obtaining the values of sheet parameters in this way, its length can also be calculated from the following equation

$$L = \sqrt{(H-h)^2 + b^2} \qquad (20)$$

To find the values of the parameters, it is necessary to have zero points (x_0, x(min), x(max), x_1, x_2) shown in the mathematical equations, sousing these points and mathematical formulas, the sheet parameters are obtained.

1.2. Synthetic Data

To prove the correctness of complex gradient method, first the data obtained from synthetic models are used. In order to create synthetic data, several synthetic data items are created with predefined parameters. The models No. 1 and 2 with constant dip angle and dipole moment at different depths, and models No. 3 and 4 with constant dipole moment and depths with different dip angle are considered.

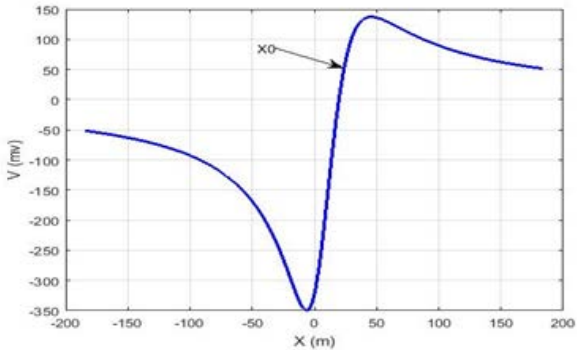

Figure 2: Self-Potential Anomaly Due to Synthetic Model 2 Without Noise.

Table 1: Parameters of synthetic models and results of the present method

Artificial Models	h(m)	H(m)	θ (degree)	K (mv)
1-9=h, 18= H θ=25 , K=250	9.0000	18.0000	25.0000	250.0006
2-17=h, 26= H θ=25 , K=250	17.0000	26.0000	25.0000	250.0007
3-3=h, 8= H θ=10 , K=100	2.9999	7.9999	9.9999	100.0001
4-3=h, 8= H θ=70 , K=100	3.0002	7.9937	70.0124	100.0282

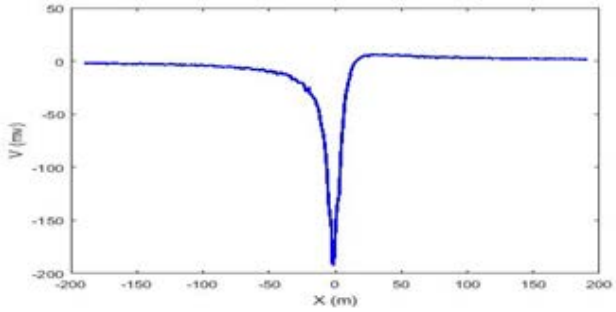

Figure 3: Self-Potential Anomaly Due to Synthetic Model 4 with Noise.

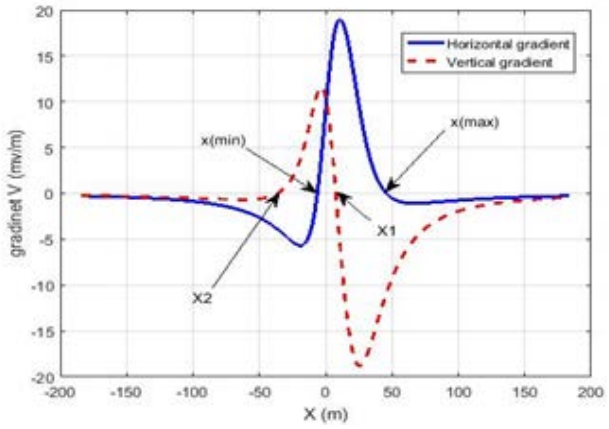

Figure 4: Complex Gradient Anomaly for Self-Potential Anomaly Described in Figure. 2.

Placing these parameters in equation allows the computation of potentials for various x_i plotted in the without-noise state in Figure 2. Then, by applying the complex gradient method of Figure 3 to calculate zero points (x_0, x(min),x-(max), x_1, x_2), a program is written that calculates these points automatically. Thus, the parameters of depth to upper edge, depth to lower edge, dip angle and electric dipole moment are obtained using mathematical Equation 12, 15, 16, 17, 18, 19. The results of using synthetic models' synthetic data are shown in Table 1. As can be seen from the Table 1, the parameters calculated are almost the same as input parameters; therefore, the correctness of this method is proved for this synthetic model. Now, we try the complex gradient method for synthetic data with noise. We randomly added 10% of noise to the data generated in the mentioned models shown in Figure 4.

Table 2: Parameters of synthetic models and the results of the present method with ±10% noise to synthetic data.

Artificial models	H(m)	percentage error h	H(m)	percentage error H	θ (□□□□)	percentage error θ	K (mv)	percentage error k
9=h, 18= 1: H θ=25 , K=250	9.504	0.56	18.2990	1.66	25.1632	0.6	228.6295	8.54
17=h, 26= 2: H θ=25 , K=250	17.2848	2.84	26.3762	1.44	25.2709	1.08	268.7131	7.4
3=h, 8= 3: H θ=10 , K=100	3.0212	0.706	7.9776	0.28	10.1400	1.4	98.0284	1.97
3=h , 8= 4: H θ=70 , K=100	3.0510	1.7	7.2512	9.36	71.7588	2.51	106.4341	6.43

Similar to the without noise state, we estimate the model parameters. In table 2 the results are collected and the error percentage of each parameter is also calculated. Finally, by plotting the curve of the data which noise added has been using the estimated parameters, the correctness of this method is proved on this synthetic model with the noise.

1.3. Field Data

Now that the method used calculates the parameters correctly. Then, the described algorithm is applied to the actual data collected. In the article, they worked on a graphite mine in southern Bavarian woods, Germany [12]. Again, the modified method is applied to this area to ensure the algorithm also is applied to other two areas of the copper mine in the Surda, India, and the cooper sulfide mine in the Suleymankoy, Turkey.

The copper mine in the Surda, India: Figure 5 shows the SP anomaly for a copper mine in the Surda, India, studied by [14]. First, we determine the origin using analytical signal because we do not know the source location when taking data; then, we apply complex gradient method to the data extracted from this mine in Figure 6, the parameters of the cause of this anomaly. We obtain z by calculating the depth from the model center as half the sum of the bottom edge depth and the upper edge depth. The results are shown in Table 3.

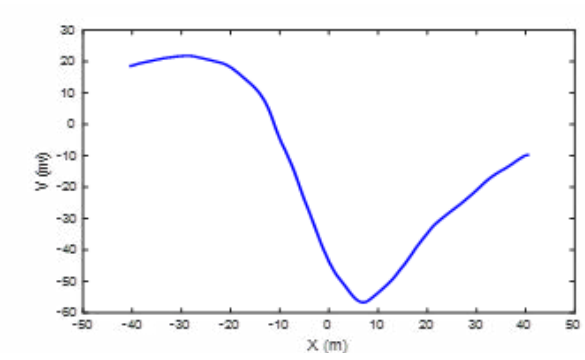

Figure 5: Self-Potential Anomaly Due to Copper Mine in the Surda, India

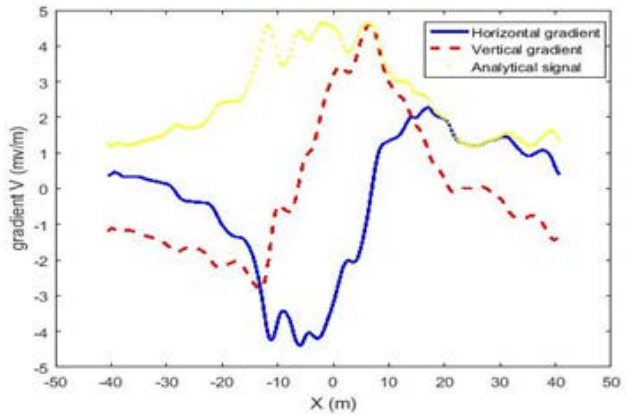

Figure 6: Complex Gradient for the SP Anomaly Described in Figure 4.

Table 3: Estimated Parameters of Copper Mine in the Surda, India.

H (m)	H (m)	Z (m)	θ (°)	K (mv)	L (m)
14.1578	16.2124	15.1851	-31.9223	133.1863	3.8857

The observed potential curve and the evaluated potential using the method explained in this thesis are shown in Figure 7. Here, there is a good closeness between the observed and evaluated data, the error of this method is estimated on this data.

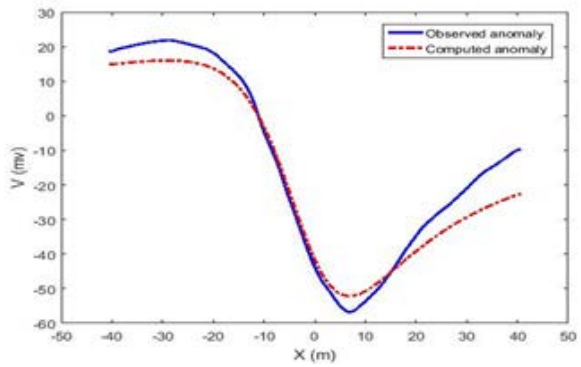

Figure 7: Observed and Calculated Potential Computed Anomaly Due to a Copper Mine in Surda, India with error % 7.1626

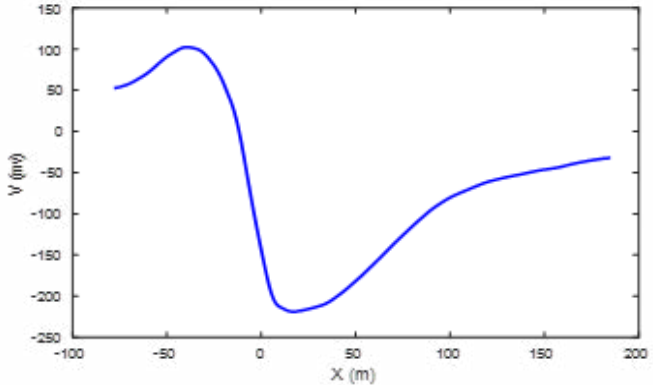

Figure 8: SP Anomaly Due to Copper Sulfide Mine in the Suleymankoi, Turkey.

the cooper sulfide mine in the suleymankoy, Turkey. studied the SP anomaly of the cooper mine suleymankoi, turkey [15]. Figure 8 is the observed data related to this mine. We apply complex gradient method to the data extracted from this mine in Figure 9. the parameters related to the cause of this anomaly have been obtained, and z calculates the depth from the center of the model as half the sum of the lower edge depth and the upper edge depth. The results are shown in Table 4.

The observed potential curve and the evaluated potential using the method stated in this thesis are shown in Figure 10. As can be seen in Figure 10, there is a good closeness between the observed and evaluated data, the error of this method is estimated on this data.

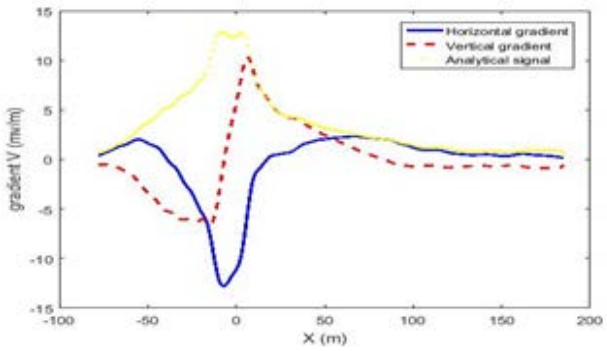

Figure 9: Complex Gradient for the SP Anomaly Described in fig 7.

Table 4: Estimated Parameters of Copper Mine in the Suleymankoy, Turkey.

h (m)	H (m)	Z (m)	θ (°)	K (mv)	L (m)
26.0407	27.9616	27.0011	-18.1046	770.7984	6.1816

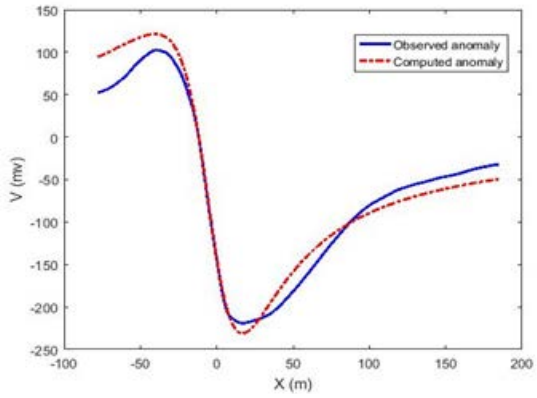

Figure 10: Observed and Calculated Potential Computed Anomaly Due to a Copper Sulfide Mine in the Suleymankoy, Turkey with Error %5.7967

The graphite mine in the southern Bavarian woods, Germany in 1962, the graphite mine in the southern Bavarian woods, Germany, was studied by Meiser. He attributed the anomaly to a polarized sheet. Figure 11 shows the SP anomaly measured in this mine. We apply complex gradient method to the data extracted from this mine in Figure 12. The parameters of the cause of this anomaly were obtained, and z calculates the depth from the center of the model as half the sum of the lower edge depth and the upper edge depth. The results are shown in Table 5. The depth obtained from the present method is very close to the depth derived (z=53). According to the results shown in the table, a good closeness is observed between the present method and other methods. good closeness is observed between the present method and other methods.

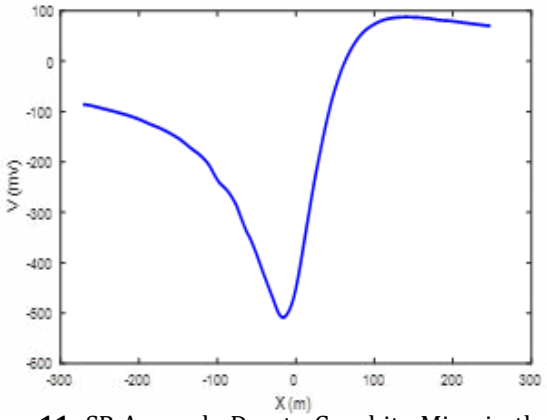

Figure 11: SP Anomaly Due to Graphite Mine in the Southern Bavarian Woods, Germany.

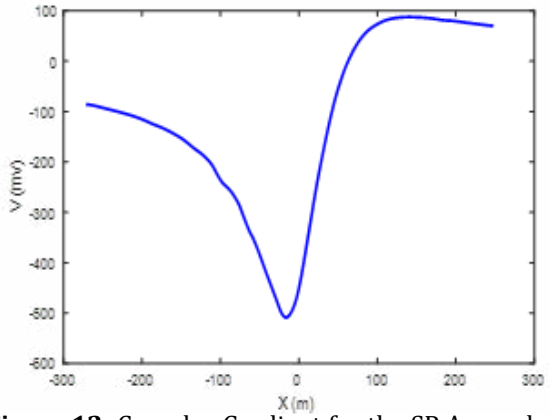

Figure 12: Complex Gradient for the SP Anomaly Described in figure 9

Table 5: Estimated Parameters of Graphite Mine in the Southern Bavarian Woods, Germany.

h (m)	H (m)	Z (m)	θ (°)	K (mv)	L (m)
33.1483	64.7953	48.9718	49.2773	336.4162	41.7575

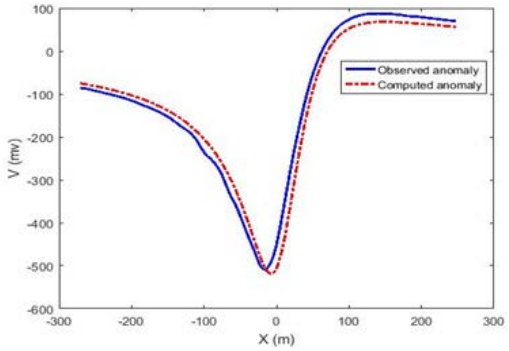

Figure 13: Observed and Calculated Potential Computed Anomaly Due to a Graphite Mine in The Southern Bavarian Woods, Germany with Error 4.7171%.

In figure 13, we can evaluate the observed anomaly which are the same as the computed anomaly obtained from the parameters of this method with an error of 4.7171%. The results are shown in Table 6. The depth obtained from the present method is very close to the depth derived (z=53). According to the results of the table, a good closeness is observed between the present method and other methods.

Table 6: Comparison of Complex Gradient Method with Other Methods Performed on Bavarian Graphite my Data.

parameters	Meiser (1962)	Abdelrahman et al (1999)	Abdelrahman et al (2001)	Present method
h (m)	34	35.8	25.2	33.1483
H (m)	72	66.3	70.8	64.7953
θ (°)	46	49.5	44.5	49.2775
K (mv)	-	363	216	336.4162
Z (m)	53	51	48	48.9718

2. Conclusion

in this paper, it was proved that the complex gradient method is a fast and simple way to interpret the SP anomaly, in which the two dimensional inclined sheet model relation were used to estimate the cause of SP anomaly parameters and thus the two-dimensional inclined sheet proved to be a suitable model for describing the cause of sp anomaly the correctness of this method was also proved on synthetic data by changing depths and changing angles and its efficiency was proved by applying this method to field example and it was observed that the error between the model data and the real data has an acceptable value, which shows that the method of this dissertation can provide models that its data should be close to the observed data and there should be a small error between them [16-20]. also, in the study of the inclined sheet model, it was proved that such a model can be

considered as a mass of spontaneous potential source, but the the real underground model can not be considered exactly a two-dimensional inclined sheet.

References

1. Zhu, Z., Tao, C., Shen, J., Revil, A., Deng, X., et al. (2022). Self-potential investigation of a deep-sea polymetallic sulfide deposit at the Southwest Indian Ridge (Indian Ocean). Authorea Preprints.
2. Alarouj, M., & Jackson, M. (2019, June). Monitoring Fluid Flow in Oil Reservoirs Using Downhole Measurements of Self-Potential. In 81st EAGE Conference and Exhibition 2019 (Vol. 2019, No. 1, pp. 1-5). European Association of Geoscientists & Engineers.
3. Hu, K., Huang, Q., & Xue, L. (2020). Groundwater Flow Monitoring by Fusion Probability Tomography of Self-Potential Data. IEEE Geoscience and Remote Sensing Letters, 18(4), 587-591.
4. Gobashy, M., Abdelazeem, M., Abdrabou, M., & Khalil, M. H. (2020). Estimating model parameters from self-potential anomaly of 2D inclined sheet using whale optimization algorithm: applications to mineral exploration and tracing shear zones. Natural Resources Research, 29, 499-519.
5. Eppelbaum, L. V. (2020). Quantitative analysis of self-potential anomalies in archaeological sites of Israel: an overview. Environmental Earth Sciences, 79(15), 377.
6. Constable, S., Kowalczyk, P., & Bloomer, S. (2018). Measuring marine self-potential using an autonomous underwater vehicle. Geophysical Journal International, 215(1), 49-60.
7. Biswas, A., & Sharma, S. P. (2017). Interpretation of self-potential anomaly over 2-D inclined thick sheet structures and analysis of uncertainty using very fast simulated annealing global optimization. Acta Geodaetica et Geophysica, 52, 439-455.
8. Di Bello, G., Lapenna, V., Satriano, C., & Tramutoli, V. (1994). Self-potential time series analysis in a seismic area of the Southern Apennines: preliminary results.
9. Abdelrahman, E. S. M., Essa, K. S., Abo-Ezz, E. R., Sultan, M., Sauck, W. A., et al. (2008). New least-squares algorithm for model parameters estimation using self-potential anomalies. Computers & Geosciences, 34(11), 1569-1576.
10. Di Maio, R., Piegari, E., Rani, P., Carbonari, R., Vitagliano, E., et al. (2019). Quantitative interpretation of multiple self-potential anomaly sources by a global optimization approach. Journal of Applied Geophysics, 162, 152-163.
11. Abdelrahman, E. M., Hassaneen, A. G., & Hafez, M. A. (1998). Interpretation of self-potential anomalies over two-dimensional plates by gradient analysis. pure and applied geophysics, 152, 773-780.
12. Hafez, M. A., & Abbas, A. M. (2011). A new approach to interpret self-potential anomaly over a two-dimensional inclined sheet using complex gradient analysis. Arabian Journal of Geosciences, 4(5), 837-844.
13. Roy, A., & Chowdhury, D. K. (1959). Interpretation of self-potential data for tabular bodies. Journal of Scientific and Engineering Research, 3, 35-54.
14. Murthy, B. V. S., & Haricharan, P. (1984). Self-potential anomaly over double line of poles—interpretation through log curves: Proceedings of the Indian Academy of Science (Earth and Planetary Science).
15. Yungul, S. H. (1950). Interpretation of spontaneous polarization anomalies caused by spheroidal ore bodies. Geophysics, 15(2), 237-246.
16. Abdelrahman, E. M., Hassaneen, A. G., & Hafez, M. A. (1999). A least-squares approach for interpretation of self-potential anomaly over a two-dimensional inclined sheet. Arabian Journal for Science and Engineering, 24(1 A), 35-42.
17. Abdelrahman, E. M., Hassaneen, A., & Hafez, M. A. (2001). A new leastsquares minimization approach to depth determination from numerical horizontal self-potential gradient over a 2-D inclined sheet. KUWAIT JOURNAL OF SCIENCE AND ENGINEERING, 28(2), 403-413.
18. Vogt, C., Klitzsch, N., & Rath, V. (2014). On self-potential data for estimating permeability in enhanced geothermal systems. Geothermics, 51, 201-213.
19. Zakaria, M. T., Muztaza, N. M., Olugbenga, A. T., Saad, R., & Rahman, M. N. A. (2020). Self-potential and 2-D resistivity application for groundwater exploration in fractured reservoirs. Songklanakarin Journal of Science & Technology, 42(2).
20. Chaput, M., Finizola, A., Peltier, A., Villeneuve, N., Crovisier, M., et al. (2019). Where does a volcano break? Using self-potential reiteration to forecast the precise location of major destructive events on active volcanoes: the case study of the Piton de la Fournaise 2007 caldera collapse. Volcanica, 2(2).